energies

Article

A Class of Control Strategies for Energy Internet Considering System Robustness and Operation Cost Optimization

Haochen Hua [1], Chuantong Hao [1], Yuchao Qin [1], and Junwei Cao [1,*]

[1] Research Institute of Information Technology, Tsinghua University, Beijing, P. R. China;
* Correspondence: jcao@tsinghua.edu.cn; Tel.: +86-010-627-72260

Received: date; Accepted: date; Published: date

Abstract: Aiming at restructuring the conventional energy delivery infrastructure, the concept of energy Internet (EI) has been popular in recent years. Outstanding benefits from an EI include openness, robustness and reliability. Most of the existing literatures focus on the conceptual design of EI, lack of theoretical investigation on developing specific control strategies for the operation of EI. In this paper, a class of control strategies for EI considering system robustness and operation cost optimization is investigated. Focusing on the EI system robustness issue, system parameter uncertainty, external disturbance and tracking error are taken into consideration, and we formulate such robust control issue as a structure specified mixed H_2/H_∞ control problem. When formulating the operation cost optimization problem, three aspects are considered: realizing the bottom-up energy management principle, reducing the purchasing cost of electricity from power grid (PG), and avoiding the situation of over-control. We highlight that this is the very first time that the above targets are considered simultaneously in the field of EI. The integrated control issue is considered in frequency domain and is solved by particle swarm optimization (PSO) algorithm. Simulation results show that our proposed method achieves the integrated control targets.

Keywords: energy Internet; microgrids; mixed H_2/H_∞ control; optimal control; robust control;

1. Introduction

Over the last few decades, global warming, energy crisis and ecological issues have promoted the research of renewable power generation and distributed energy networks [1,2]. For the integration of a variety of distributed energy resources (DERs), microgrids (MGs) play an important role [3,4]. In MGs, the produced power by renewable energy sources (RESs) including photovoltaic (PV) units and wind turbine generators (WTGs) has disadvantages such as low inertia, uncertainty, and dynamic complexity [5,6]. Besides, the output power of electrical loads depends on residents' power usage customs and varies stochastically [7]. In MGs, to alleviate power imbalance, and to regulate voltage/frequency oscillation, the control of MGs is a subject of both practical and theoretical importance [8].

Following the principle of smart grid specializing in informatization and intellectualization of the existing power systems [9], and to solve the aforementioned challenges within the scenario of multiple interconnected MGs, the new concept of energy Internet (EI) is proposed [10] and is considered to be an upgraded version of smart grid [11]. Inspired by cores of Internet, the EI solves energy related problems by integrating bi-directional flows of information and power [12]. In an EI scenario, multiple MGs are interconnected via energy routers (ERs) [13] which are also known as energy hubs [14], or power routers [15]. Different from the top-down mode in the existing power systems, bottom-up is a fundamental energy management principle in EI [11]. To achieve such target, each individual MG in EI shall be able to regulate the power deviation with its local energy storage, generation and consumption devices with priority. If power balance in any MG is hard to be achieved autonomously, other MGs can send/absorb electrical energy to/from it via ERs, helping achieve its local power balance [11]. Significant benefits from an EI include openness, robustness and reliability [12].

In the field of EI, when multiple MGs are interconnected, the related energy management and control issues are more complicated than the ones in MGs. Optimal control problems regarding energy management have been popular. For example, coordinated optimal control algorithm for smart distribution management system in multiple MGs is investigated in [16]. Applying multi-objective stochastic optimization approach to solve the optimal energy management issues in MGs has been reported in [17]. To achieve an optimized operation of an off-grid MG, nonlinear droop relations are implemented [18]. In [19], optimal control strategy for MG under both off-grid and grid-connected mode has been studied. Distributed control and optimization in DC MGs is investigated in [20].

On the other hand, robust control problems in the field of MG and EI has received much attention in the past few years. For instance, in [21], both H_∞ and μ-synthesis approaches are utilized to regulate AC bus frequency deviations in an off-grid MG. The stochastic H_∞ control theory is applied to solve the coordinated frequency control problem within an EI scenario in [22]. In [23], the issue of voltage control in an EI scenario is formulated as a non-fragile robust H_∞ control problem regarding an uncertain stochastic nonlinear system, and it is solved via linear matrix inequality approach. Robust H_∞ load frequency control in hybrid distributed generation system has been studied in [24].

When both optimal and robust control problems are considered simultaneously, the application of mixed H_2/H_∞ control theory for MGs has attracted much attention, and significant advances on this topic have been made. For an islanded AC MG, the problems of operation cost optimization and frequency regulation are formulated as a mixed H_2/H_∞ control problem in deterministic and stochastic systems in [25] and [26], respectively. It has been shown that the fixed structure mixed H_2/H_∞ control technique can be used to obtain a coordinated vehicle-to-grid control and frequency controller for robust load-frequency control (LFC) in a smart grid [27]. A robust mixed H_2/H_∞ based LFC of a deregulated power system including superconducting magnetic energy storage has been proposed in [28]. For other works regarding the application of mixed H_2/H_∞ control into MGs, readers can refer to [29,30], etc. It is notable that although mixed H_2/H_∞ control technique has been widely used in conventional power systems, there has been few working applying such control schemes into the field of EI.

When multiple MGs are interconnected via ERs, no matter they are grid-connected or not, there are a variety of optimal and robust control problems worth considering. In this paper, we are concerned with the problems of controller design for EI considering system robustness and operation cost optimization. A series-shaped EI is studied in this article. Within the considered EI scenario, three MGs are interconnected successively and one MG has access to the main power grid (PG). In MGs, we assume that there exist the following elements: PV units, WTGs, fuel cells (FCs), hydrogen tanks (HTs), electrolyzer (ES), micro-turbines (MTs), heat pump (HPs), plug-in hybrid electric vehicle (PHEVs), diesel engine generators (DEGs), battery energy storage (BES) devices, flywheel energy storage (FES) devices, ERs and normal loads. The system of EI is formulated via frequency domain approach. When the above robust and optimal control targets are considered simultaneously, proportional integral (PI) controllers are utilized in ESs, MTs, HPs, PHEV, DEGs, and the transmission line between MG_1 and MG_2 and the transmission line between MG_2 and MG_3. Then, we solve such control problem via particle swarm optimization (PSO) algorithm [31]. Next, simulations demonstrate the usefulness and effectiveness of our proposed controller.

The importance and contribution of this work can be outlined as follows. As is mentioned above, some existing works only investigates either robustness or operation cost optimization of the EI systems. In this paper, this is the very first time that both two aspects are considered *simultaneously* in the field of EI, rather than in conventional energy systems. Our work can be viewed as an extension as well as a generalized version for the ones focusing on single islanded or grid-connected MG.

Compare this paper with some existing ones adopting time domain approach (e.g., [7,22,23,25,26]), our work formulated in frequency domain has the advantage that it is convenient to be implemented in actual dynamic situations. With the proposed controller, the following targets are achieved *simultaneously*. 1) The system robustness against parameter uncertainty and external disturbance is achieved. 2) The tracking error is controller to a relative low level. 3) The bottom-up energy management principle is achieved, such that an autonomous power balance in each MG is achieved with priority. 4) The effect of electricity market price is considered, and the purchasing cost of electricity from PG is restricted. 5) The controllable devices in MGs is utilized rationally, and the situation of over-control is avoided. 6) Considering different preferences of the system manager, the importance of each control target can be adjusted by changing the size of its corresponding weighting coefficient. 7) In simulation results, it is shown that the proposed controller performs better than the conventional ones do. It is highlighted that our work is of both theoretical and practical importance.

The rest of the paper is organized as follows: Section 2 introduces the system modelling. The control problem is formulated and solved in Section 3. Section 4 presents some simulations. Finally, some conclusions are drawn in Section 5.

2. System Modelling

In this section, we focus on a series-shaped EI system with three ERs. Every component of the system is modeled with first order transfer function in frequency domain. Then, an explicit mathematical control system is obtained.

2.1. The Scenario of an EI

A series-shaped EI is studied in this article. MG_1, MG_2 and MG_3 are connected successively. Besides, we assume that MG_1 is connected to PG. All the ERs are designed to be based on AC bus lines. Figure 1 shows the topology of the studied EI system.

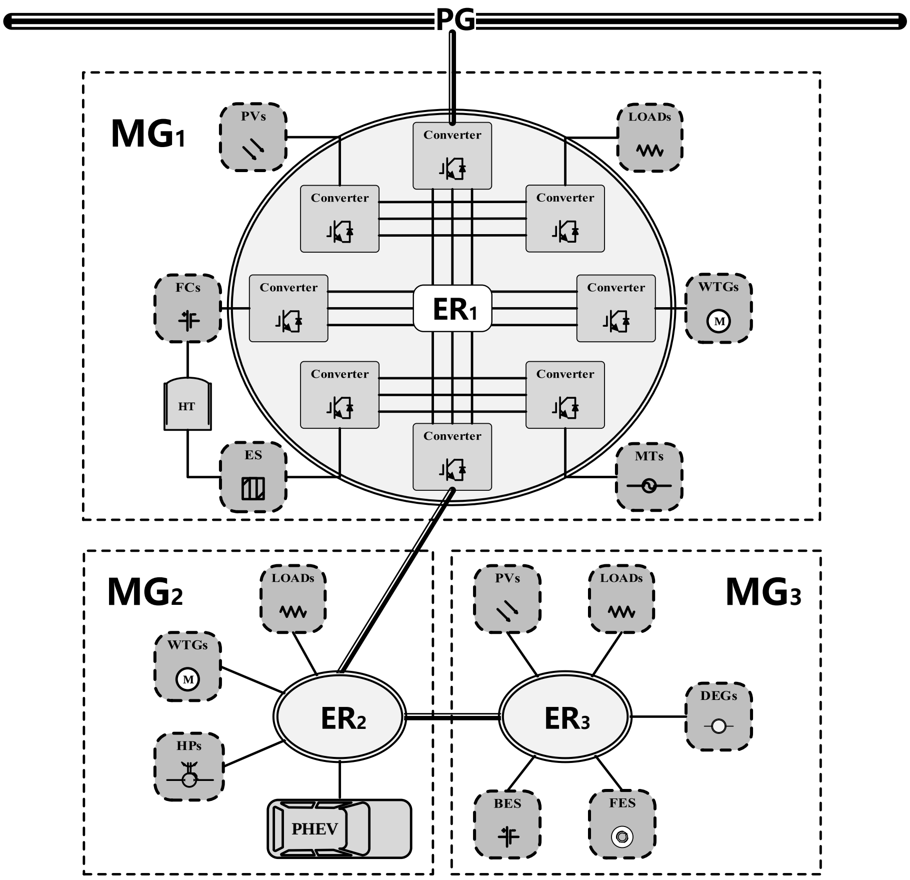

Figure 1. The studied series-shaped EI system.

In $\mathrm{MG_1}$, PV units, WTGs, loads, FCs, MTs, HTs and ESs are connected to $\mathrm{ER_1}$ via converters. The main power supply in $\mathrm{MG_1}$ is assumed to reply on power output by PV units and WTGs. If the power generation by PV units and WTGs is not enough for power consumption in $\mathrm{MG_1}$, highly controllable power generators such as MTs and FCs are utilized to fill the power supply-demand gap. Whenever there exists superfluous energy in $\mathrm{MG_1}$, ESs are used to covert electric energy into hydrogen which is stored in HTs. Hydrogen can be used to generate power by FCs. Normal loads such as housings or factories have access to $\mathrm{ER_1}$, as well. Besides, $\mathrm{MG_1}$ is designed to have connection to PG and $\mathrm{ER_2}$.

$\mathrm{MG_2}$ is designed to have access to different components in $\mathrm{MG_1}$, except for the requisite local loads. WTGs are utilized as the major power generators in $\mathrm{MG_2}$. We assume that in residential communities and cluster charging stations, large amounts of highly controllable HPs and PHEVs are connected to $\mathrm{ER_2}$. When the power generation is larger than consumption in $\mathrm{MG_2}$, the access of HPs and PHEVs shall be able to ensure the power balance of $\mathrm{MG_2}$. Whenever $\mathrm{MG_2}$ is lack of electricity, power can be transmitted from $\mathrm{MG_1}$ and $\mathrm{MG_3}$ via $\mathrm{ER_1}$ and $\mathrm{ER_2}$, respectively.

We assume that $\mathrm{MG_3}$ is only connected with $\mathrm{MG_2}$ and these two MGs are far away from each other. Thus, the dynamic response of power transmission line is slower than that of local devices in $\mathrm{MG_3}$. Assuming that $\mathrm{MG_3}$ is sensitive to power deviation, responsive energy storage devices such as BES and FES are essential to keep its power balance. Besides, another kind of highly controllable power generators, DEGs, have connection with $\mathrm{MG_3}$. PV units and loads are also included in $\mathrm{MG_3}$.

2.2. Linearized Block Diagram

First, let us introduce the following notations. The frequency deviations of $\mathrm{MG_1}$, $\mathrm{MG_2}$ and $\mathrm{MG_3}$ are denoted as Δf_1, Δf_2 and Δf_3, respectively. The power deviations of AC buses in $\mathrm{MG_1}$, $\mathrm{MG_2}$ and $\mathrm{MG_3}$ are denoted as ΔP_1, ΔP_2 and ΔP_3, respectively. Output power of PVs, WTGs, FCs and MTs in $\mathrm{MG_1}$ are denoted as P_{PV1}, P_{WTG1}, P_{FC} and P_{MT}, respectively. Output power of WTGs in $\mathrm{MG_2}$ and PVs in $\mathrm{MG_3}$ are denoted as P_{WTG2} and P_{PV3}, respectively. Power consumption of loads in $\mathrm{MG_1}$, $\mathrm{MG_2}$ and $\mathrm{MG_3}$ are denoted as P_{LOAD1}, P_{LOAD2} and P_{LOAD3}, respectively. The output power of ESs, FCs, MTs, HPs, PHEVs and DEGs are denoted as P_{ES}, P_{FC}, P_{MT}, P_{HP}, P_{PHEV} and P_{DEG}, respectively. Exchange power of BES and FES devices are denoted as P_{BES} and P_{FES}, respectively. P_{PG}, P_{ER12} and P_{ER23} represent the power transmission between PG and $\mathrm{MG_1}$, between $\mathrm{MG_1}$ and $\mathrm{MG_2}$ and between $\mathrm{MG_2}$ and $\mathrm{MG_3}$, respectively.

Power balance equation of $\mathrm{MG_1}$, $\mathrm{MG_2}$ and $\mathrm{MG_3}$ can be expressed in (1), (2) and (3), respectively:

$$\Delta P_1 = P_{PV1} + P_{WTG1} + P_{FC} + P_{MT} + P_{PG} - (P_{ES} + P_{ER12} + P_{LOAD1}), \quad (1)$$

$$\Delta P_2 = P_{WTG2} + P_{ER12} - (P_{PHEV} + P_{HP} + P_{ER23} + P_{LOAD2}), \quad (2)$$

$$\Delta P_3 = P_{PV3} + P_{DEG} + P_{ER23} - P_{LOAD3} \pm (P_{BES} + P_{FES}). \quad (3)$$

The change of P_{FC}, P_{MT} and P_{ES} are denoted as ΔP_{FC}, ΔP_{MT} and ΔP_{ES}, respectively. The gain of ESs, FCs, MTs, HPs and PHEVs are denoted as K_{ES}, K_{FC}, K_{MT}, K_{HP} and K_{PHEV}, respectively. The time constants of ESs, FCs, HPs, PHEVs, BES devices, FES devices and DEGs are denoted as T_{ES}, T_{FC}, T_{HP}, T_{PHEV}, T_{BES}, T_{FES} and T_{DEG}, respectively. ΔP_{ESC}, ΔP_{MTC}, U_{HP}, U_{PHEV} and U_{DEG} stand for the control outputs of ESs, MTs, HPs, PHEVs and DEGs. Damping coefficients and inertia constants in $\mathrm{MG_1}$, $\mathrm{MG_2}$ and $\mathrm{MG_3}$ are denoted as are denoted as D_1 and M_1, D_2 and M_2, D_3 and M_3, respectively. K_{MTC}, K_{ESC}, K_{HPC}, K_{PHEVC} and K_{DEGC} represent for the PI controllers of MTs, ESs, HPs, PHEVs and DEGs, respectively. Moreover, T_{ER12}, U_{ER12} and K_{ER12C} stand for time constant, control output and PI controller of transmission line between $\mathrm{MG_1}$ and $\mathrm{MG_2}$, while T_{ER23}, U_{ER23} and K_{ER23C} stand for time constant, control output and PI controller of transmission line between $\mathrm{MG_2}$ and $\mathrm{MG_3}$. The values of b_{ER12} and b_{ER23} depend on real engineering scenarios and can be measured by parameter estimation methods [32].

In this paper, ΔP_{ES} and ΔP_{FC} are approximated by a first order transfer function [33], as is shown in (4) and (5):

$$\Delta P_{ES} = \frac{K_{ES}}{1 + T_{ES}s} \Delta f_1, \tag{4}$$

$$\Delta P_{FC} = \frac{K_{FC}}{1 + T_{FC}s} \Delta f_1. \tag{5}$$

Considering the linear power versus frequency droop characteristics, ΔP_{MT} is obtained by (6):

$$\Delta P_{MT} = -\frac{1}{K_{MT}} \Delta f_1. \tag{6}$$

Relative phase angle [rad] between PG and ER_1 is obtained by (7):

$$\theta = 2\pi f_0 \int \Delta f_1 dt. \tag{7}$$

Let us denote θ as the relative phase angle and X_{PG} as line reactance. Consequently, P_{PG} is given by (8):

$$P_{PG} = \frac{sin\theta}{X_{PG}}. \tag{8}$$

Based on previous studies [23,34], P_{HP}, P_{PHEV} and P_{ER12} are obtained by the following equations:

$$P_{HP} = \frac{K_{HP}}{1 + T_{HP}s} K_{HPC} \Delta f_2, \tag{9}$$

$$P_{PHEV} = \frac{K_{PHEV}}{1 + T_{PHEV}s} K_{PHEVC} \Delta f_2, \tag{10}$$

$$P_{ER12} = \frac{b_{ER12}}{1 + T_{ER12}s} K_{ER12C} \Delta f_2. \tag{11}$$

We assume that BES and FES devices are equipped with internal controllers and respond to the AC bus frequency deviation [21]. P_{BES} and P_{FES} can be obtained by:

$$P_{BES} = \frac{1}{1 + T_{BES}s} \Delta f_3, \tag{12}$$

$$P_{FES} = \frac{1}{1 + T_{FES}s} \Delta f_3. \tag{13}$$

P_{DEG} and P_{ER23} are obtained by equations (14) and (15):

$$P_{DEG} = \frac{1}{1 + T_{DEG}s} K_{DEGC} \Delta f_3, \tag{14}$$

$$P_{ER12} = \frac{b_{ER23}}{1 + T_{ER23}s} K_{ER23C} \Delta f_3. \tag{15}$$

Rapid or oversized power deviation may lead to instability of the AC bus frequency oscillation in MGs. With desired control strategies in MG_1, MG_2 and MG_3, power balance in these MGs can be achieved, and instability of Δf_1, Δf_2 and Δf_3 can be avoided. In this paper, PI controllers are utilized on ESs, MTs, HPs, PHEV, DEGs, and the transmission line between MG_1 and MG_2 and the transmission line between MG_2 and MG_3. Then, we have:

$$\begin{cases} \Delta P_{ESC} = K_{ESC}(s) \cdot P_{PG}, \\ \Delta P_{MTC} = K_{MTC}(s) \cdot P_{PG}, \\ U_{ER12} = K_{ER12C}(s) \cdot \Delta f_2, \\ U_{HP} = K_{HPC}(s) \cdot \Delta f_2, \\ U_{PHEV} = K_{PHEVC}(s) \cdot \Delta f_2, \\ U_{DEG} = K_{DEGC}(s) \cdot \Delta f_3, \\ U_{ER23} = K_{ER23C}(s) \cdot \Delta f_3. \end{cases} \tag{16}$$

where

$$
\begin{cases}
K_{ESC}(s) = K_{P_{ES}} + K_{I_{ES}}/s, \\
K_{MTC}(s) = K_{P_{MT}} + K_{I_{MT}}/s, \\
K_{ER12C}(s) = K_{P_{ER12}} + K_{I_{ER12}}/s, \\
K_{HPC}(s) = K_{P_{HP}} + K_{I_{HP}}/s, \\
K_{PHEVC}(s) = K_{P_{PHEV}} + K_{I_{PHEV}}/s, \\
K_{DEGC}(s) = K_{P_{DEG}} + K_{I_{DEG}}/s, \\
K_{ER23C}(s) = K_{P_{ER23}} + K_{I_{ER23}}/s.
\end{cases}
$$

According to (1), (4)-(8) and (16), the linearized block diagram of MG_1 is illustrated in Figure 2. According to (2), (9)-(11) and (16), the linearized block diagram of MG_2 is illustrated in Figure 3. According to (3), (12)-(15) and (16), the linearized block diagram of MG_3 is illustrated in Figure 4.

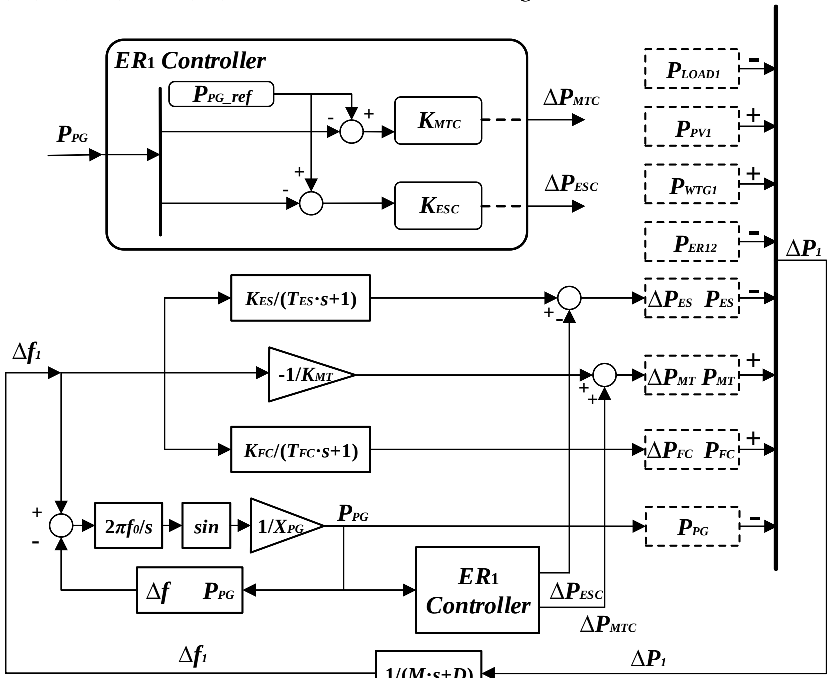

Figure 2. The linearized block diagram of MG_1.

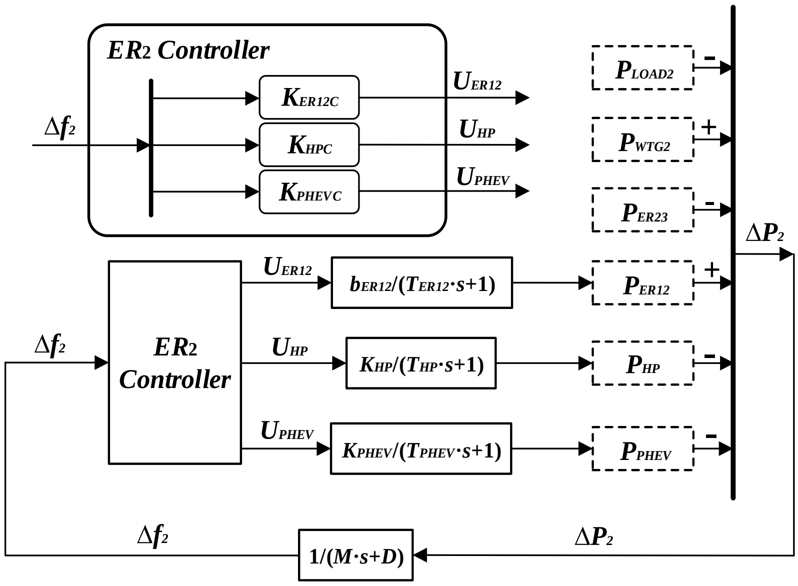

Figure 3. The linearized block diagram of MG_2.

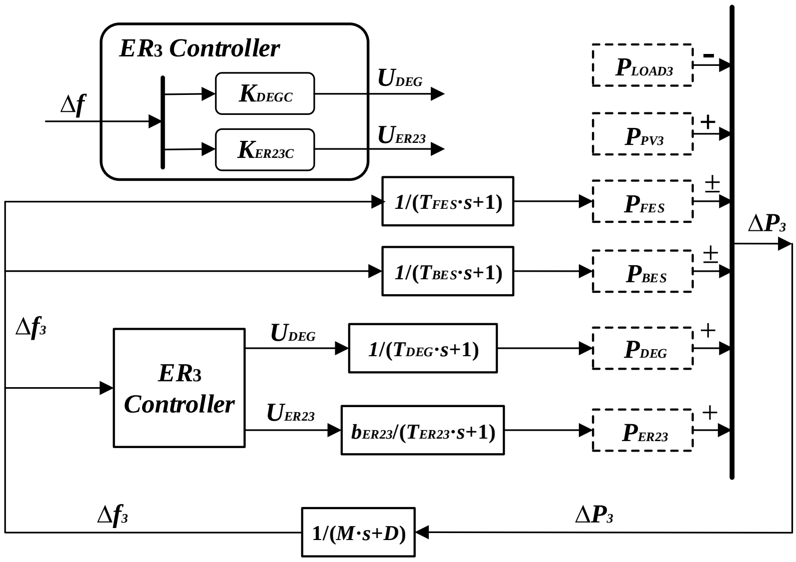

Figure 4. The linearized block diagram of MG_3.

Based on inverse Laplace transformation and the frequency-domain block diagram in Figure 2, Figure 3 and Figure 4, we are able to transform the studied EI system from (1) to (16) into an explicit mathematical control system:

$$\begin{cases} \dot{x} = Ax + Bu, \\ y = Cx + Du, \end{cases} \tag{17}$$

where x is state vector, y is output vector and u is control output, expressed as:

$$x = [\Delta P_{ES} \quad P_{PG} \quad \Delta f_1 \quad P_{HP} \quad P_{PHEV} \quad P_{ER12} \quad \Delta f_2 \quad P_{DEG} \quad P_{ER23} \quad \Delta f_3]',$$

$$y = [\Delta f_1 \quad \Delta f_2 \quad \Delta f_3]',$$

$$u = [\Delta P_{MTC} \quad \Delta P_{ESC} \quad U_{ER12} \quad U_{HP} \quad U_{PHEV} \quad U_{DEG} \quad U_{ER23}]'.$$

The EI system (16) is a multi-input-multi-output (MIMO) control system with the nominal plant G and the controller K.

In [22], it is pointed out that various topologies of EI (e.g., series-shaped, annular-shaped, star-shaped, etc.) can be formulated into mathematical systems in forms of (17). Hence, we emphasis that the investigation to series-shaped EI and the obtained results can be extended and applied into generalized EI scenarios.

3. Problem Formulation and Solution

In this section, the EI system robustness issue is formulated as the structure specified mixed H_2/H_∞ control problem, whereas the operation cost management issue in EI is formulated as a multi-objective optimization problem. We consider such mixed robust and optimal control targets simultaneously, and we solve this control problem via PSO algorithm [31].

3.1. Robust Control for EI

For a practical system, parameter measurement error and various power oscillation are inevitable, which brings system uncertainties [25] [26]. Besides, power generated by PVs depends heavily on the condition of light intensity and power generated by WTGs depends heavily on the condition of wind power. Moreover, varieties of power consumption devices can change the dissipation of power. Thus, external disturbance to the system shall be taken into consideration when designing robust controllers.

Consider a MIMO control system with external disturbances and system uncertainties, nominal plant of the studied EI is denoted as G, and K represents the proposed controller. $r(t)$, $e(t)$, $u(t)$, $d(t)$ and $y(t)$ stand for reference input, tracking error, control output, external disturbance and system output, respectively. Inverse output multiplicative uncertainty [35], denoted as Δ, is utilized to model system uncertainties. System robustness and tracking performance are formulated as H_∞ and H_2 performance, respectively. The structure specified mixed H_2/H_∞ control system is shown in Figure 5.

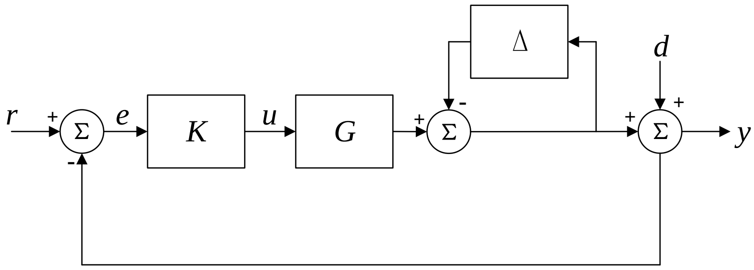

Figure 5. The control system of the studied EI with external disturbance and system uncertainties.

Based on the small gain theorem [36], a system with multiplicative uncertainties is stable if and only if (18) holds:

$$\|\Delta \cdot (I + GK)^{-1}\|_\infty < 1, \tag{18}$$

where $\|\cdot\|_\infty$ refers to the usual $\mathcal{L}_\infty[0, \infty)$ norm. So, we have

$$\|\Delta\|_\infty < \frac{1}{\|(I + GK)^{-1}\|_\infty}. \tag{19}$$

Base on (19), the size of the system uncertainties is obtained by $1/\|(I + GK)^{-1}\|_\infty$, which also implies the robust stability margin against the system uncertainties. Hence, the controlled system's robust stability is maximized when $\|(I + GK)^{-1}\|_\infty$ is minimized. The robust H_∞ control objective function is formulated as J_∞:

$$J_\infty = \|(I + GK)^{-1}\|_\infty. \tag{20}$$

In addition to robust stability and disturbance attenuation, tracking performance should be optimized as well [37]. The objective function of tracking error is formulated as the integral of the squared error:

$$J_e = \int_0^\infty e'(t)e(t)dt = \|E(s)\|_2^2. \tag{21}$$

where $\|\cdot\|_2$ stands for the usual $\mathcal{L}_2[0, \infty)$ norm, and $e(t) = r(t) - y(t)$ is the tracking error, figured out by the inverse Laplace transformation of $E(s)$ with $\Delta = 0$ and $d(t) = 0$:

$$E(s) = (I + GK)^{-1}R(s). \tag{22}$$

Thereby, considering system robustness, the structure specified mixed H_2/H_∞ control objective function is obtained by J_1 given as follows,

$$J_1 = J_e + J_\infty. \tag{23}$$

3.2. Operation Cost Optimization

The operation cost of the studied system includes varieties of aspects among which three objective functions are identified below.

The first objective is to regulate the power transmission between every two connected MGs to a relatively low level. According to the bottom-up principle for EI, the autonomous power balance in each MG shall be achieved preferably. Equivalently, power transmission P_{ER12} and P_{ER23} are expected to be kept within a relatively small amount. According to the linearized block diagrams of MG_2 and MG_3, the objective function can be formulated as J_{Trans}:

$$J_{Trans} = \left\| \frac{b_{ER12}}{1 + T_{ER12}s} K_{ER12C} \right\|_2^2 + \left\| \frac{b_{ER23}}{1 + T_{ER23}s} K_{ER23C} \right\|_2^2. \quad (24)$$

The second objective function is focused on reducing the purchasing cost of electricity from PG. Normally, the pricing of electricity fluctuates according to a number of factors; see, e.g., [38]. To illustrate, when the load power consumption is larger than power generation, the electricity price goes up, and vice versa [39,40]. Customers usually spontaneously consume more electricity when the price is at a relatively low level. If a MG relies heavily on power exchange with PG to maintain its operation, it will not only violate the energy management principles of the EI, but also lead to expensive electricity purchasing cost. Such cost is determined by the electricity price and the amount of power transmitted from PG to MG. Normally, the electricity price varies over time by hours [41]. In this article, we focus on a time slot no more than one hour. The electricity price is assumed to be constant in the case studies. The objective function is formulated as the 2-norm square of the product of electricity price and power transmitted from PG to MG_1:

$$J_{Cost} = \left\| Price_e \cdot \frac{\sin\left(\frac{2\pi f_0}{s}\right)}{X_{PG}} \right\|_2^2, \quad (25)$$

where $Price_e$ is the electricity price based on real-time electricity market.

The third objective function aims at reducing the additional cost involved by all the controllers utilized in the studied EI system. Although a stronger controller may lead to better performance, the probability of over-control is greatly increased. The situation of over-control will bring additional cost for the operation of EI. The cost function J_{Ctl} is utilized to estimate the cost involved by the controllers,

$$J_{Ctl} = \sum_{k \in \Omega} \|k\|_2^2, \quad (26)$$

where Ω is the set of all the controllers in the studied EI system. According to Section 2, we have $\Omega = \{K_{ESC}, K_{MTC}, K_{HPC}, K_{PHEVC}, K_{DEGC}, K_{ER12C}, K_{ER23C}\}$. By minimizing J_{Ctl}, the situation of over-control can be avoided effectively.

Taking three objective functions (24)-(26) and the preference of decision maker into consideration, the system operation cost function is formulated by:

$$J_2 = \omega_1 J_{Trans} + \omega_2 J_{Cost} + \omega_3 J_{Ctl}, \quad (27)$$

where ω_1, ω_2 and ω_3 are weighting coefficients.

3.3. The Mixed Control Objective

The mixed control target is described by the sum of the structure specified mixed H_2/H_∞ control objective function and the system cost optimization control objective, defined as

$$J = J_1 + J_2. \quad (29)$$

In this paper, our control target is to minimize J, subject to:

$$\begin{cases} K_{P_{min}} < K_P < K_{P_{max}} \\ K_{I_{min}} < K_I < K_{I_{max}} \end{cases}. \quad (30)$$

In (30), $K_P \in \Phi_P$ and $K_I \in \Phi_I$. Φ_P is the set of all the proportion parameters, and $\Phi_P = \{K_{P_{ES}}, K_{P_{MT}}, K_{P_{ER12}}, K_{P_{HP}}, K_{P_{PHEV}}, K_{P_{DEG}}, K_{P_{ER23}}\}$. Φ_I is the set of all the integral parameters, and $\Phi_I = \{K_{I_{ES}}, K_{I_{MT}}, K_{I_{ER12}}, K_{I_{HP}}, K_{I_{PHEV}}, K_{I_{DEG}}, K_{I_{ER23}}\}$. $K_{P_{min}}$ and $K_{P_{max}}$ are the minimum and maximum parameters of the proportion part of the controllers; $K_{I_{min}}$ and $K_{I_{max}}$ are the minimum and maximum parameters of the integral part of the controllers.

3.4. Solution to the Studied Control Problem

It is notable that the control problem described in (29)-(30) can be solved by PSO algorithm [51]. The flowchart of PSO algorithm is shown in Figure 6. The simulation results are demonstrated in the next section.

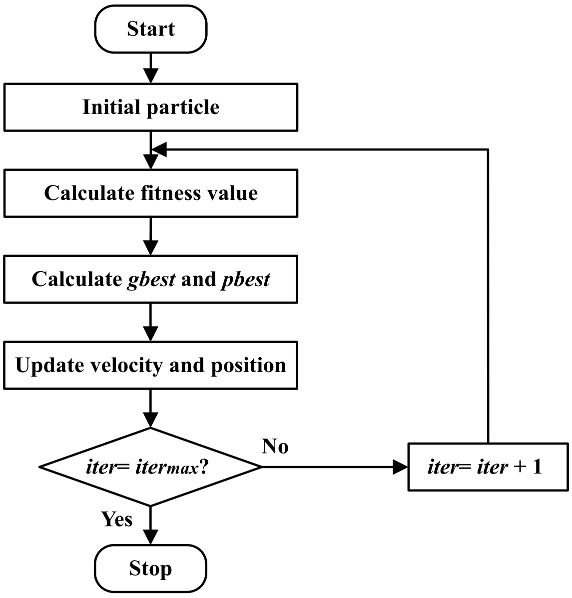

Figure 6. The flowchart of PSO algorithm.

4. Simulation Results and Analysis

In this section, some simulation results and analysis are given to verify the effectiveness of the proposed controller compared with conventional ones.

4.1. Simulation Results under the Proposed Controller

According to real engineering practice, system parameters are given in Table 1. For tracking performance, the reference input $R(s)$ in (22) is chosen to be $1/(s+5)$. The parameters of PSO algorithm are: swarm size = 50; maximum iteration = 30; c_1 = 0.2; c_2 = 0.2; w_{min} = 0.4 and w_{max} = 0.9. According to the simulation results in Figure 7, the optimized objective function value is 18.3267.

The proposed mixed H_2/H_∞ controller is:

$$\begin{cases} K_{ESC}(s) = 0.1246 + 0.2710/s, \\ K_{MTC}(s) = 0.3056 + 0.4100/s, \\ K_{ER12C}(s) = 0.4206 + 0.2710/s, \\ K_{HPC}(s) = 0.6666 + 0.2571/s, \\ K_{PHEVC}(s) = 0.3326 + 0.2948/s, \\ K_{DEGC}(s) = 0.1000 + 0.1000/s, \\ K_{ER23C}(s) = 0.7008 + 0.3066/s. \end{cases}$$

As is shown in Figure 8, the power generation by PVs and WTGs as well as the power consumption of loads in the studied EI system are assumed to be random in the investigated time period.

Table 1. System parameters.

Parameters	Value	Parameters	Value	Parameters	Value
$M_1(pu/s)$	10	K_{ES}	100	K_{MT}	0.04
$D_1(pu/Hz)$	1	$T_{ES}(s)$	60	$T_{DEG}(s)$	2
$M_2(pu/s)$	15	b_{ER12}	10	b_{ER23}	10
$D_2(pu/Hz)$	2	$T_{ER12}(s)$	1.15	$T_{ER23}(s)$	1.15

$M_3(pu/s)$	20	X_{PG}	0.072	$T_{BES}(s)$	0.15
$D_3(pu/Hz)$	1.5	$f_0(Hz)$	50	$T_{FES}(s)$	0.12
K_{HP}	10	K_{PHEV}	10		
$T_{HP}(s)$	0.2	$T_{PHEV}(s)$	0.3		

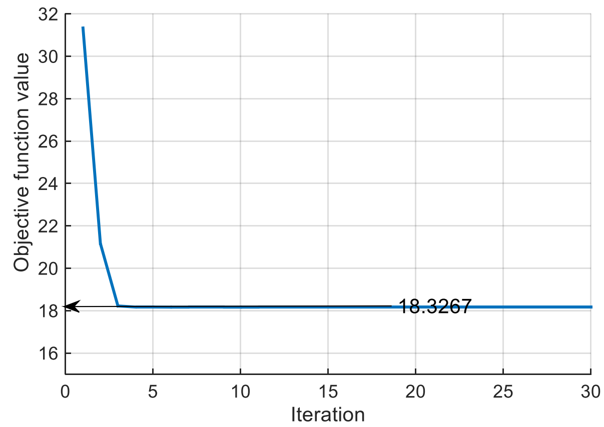

Figure 7. Objective function value.

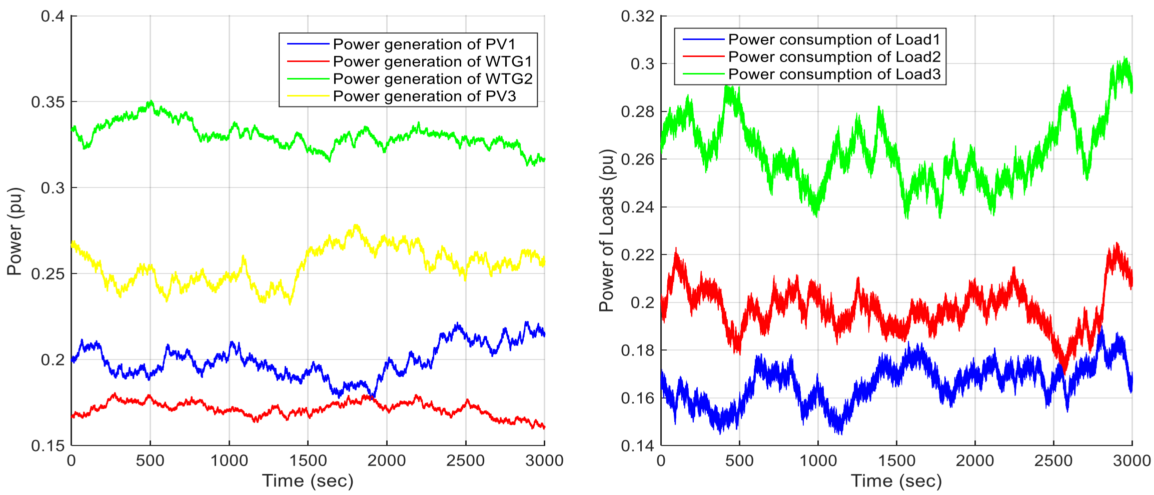

(**a**) (**b**)

Figure 8. Local power generation and consumption. (**a**) Power generation of PVs and WTGs; (**b**) Power consumption of loads.

The effect of the proposed method is compared with that of the conventional ones. Conventional methods include using only robust control which minimizes J_1 in (23) subject to (30) and using only optimal control which minimizes J_2 in (27) subject to (30).

4.2. Comparing the Proposed Controller with the Optimal Controller

First, let the conventional method be only using optimal control strategies which minimizes J_2 in (27) subject to (30).

The controlled frequency deviation of MG_1 obtained by both the proposed method and the conventional method are illustrated in Figure 9 including the following four situations: (a) without external disturbance or system parameter uncertainties, (b) with external disturbance only, (c) with system parameter uncertainties only, (d) with both external disturbance and system parameter uncertainties. The frequency deviation of MG_1 is relatively small, and the difference of the control effect of the proposed method and the conventional method is not obvious, which are due to the connection of MG_1 to PG.

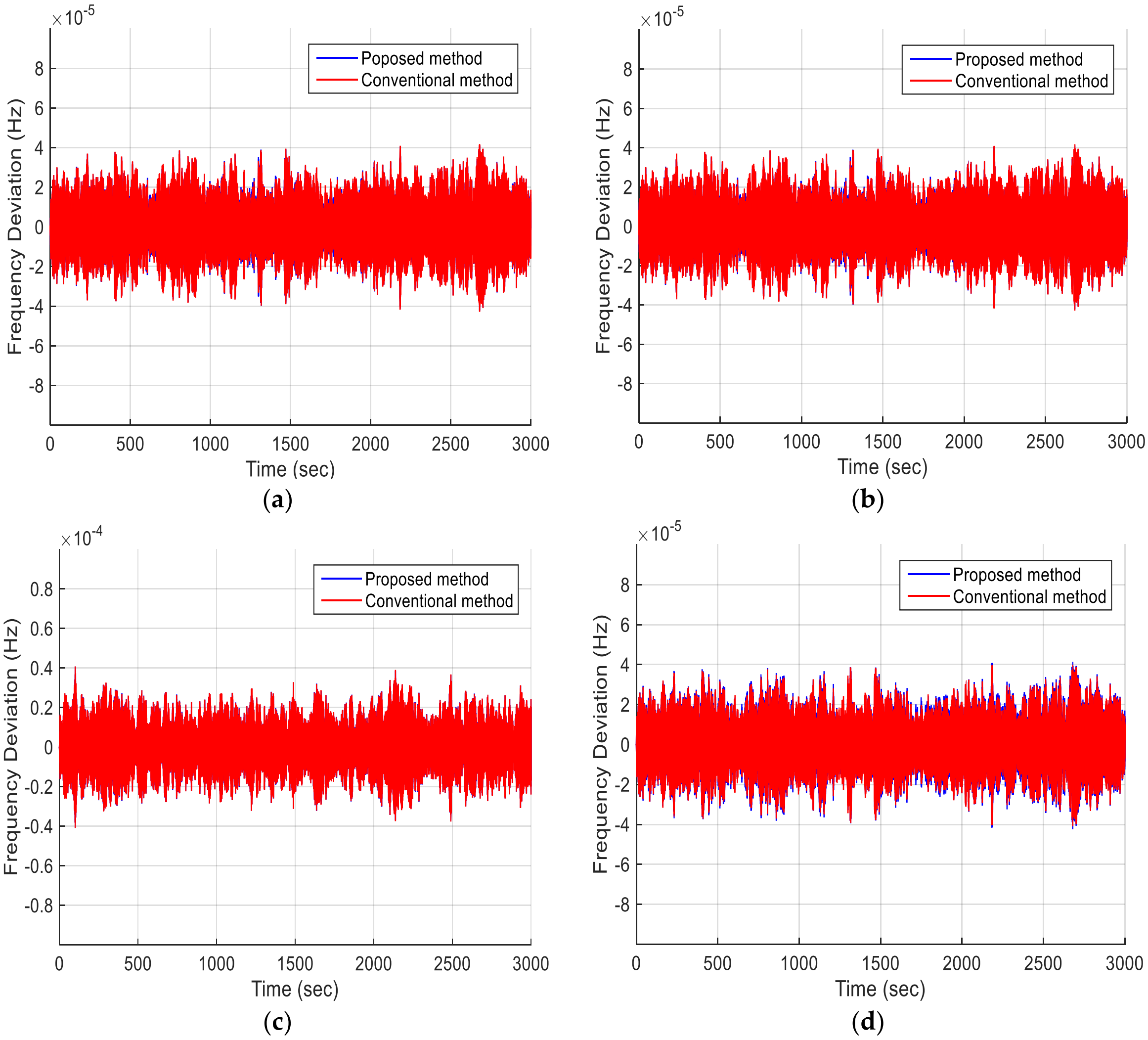

Figure 9. Frequency deviation of MG_1: (**a**) Without disturbance or uncertainties; (**b**) With external disturbance; (**c**) With system parameter uncertainties; (**d**) With external disturbance and system parameter uncertainties.

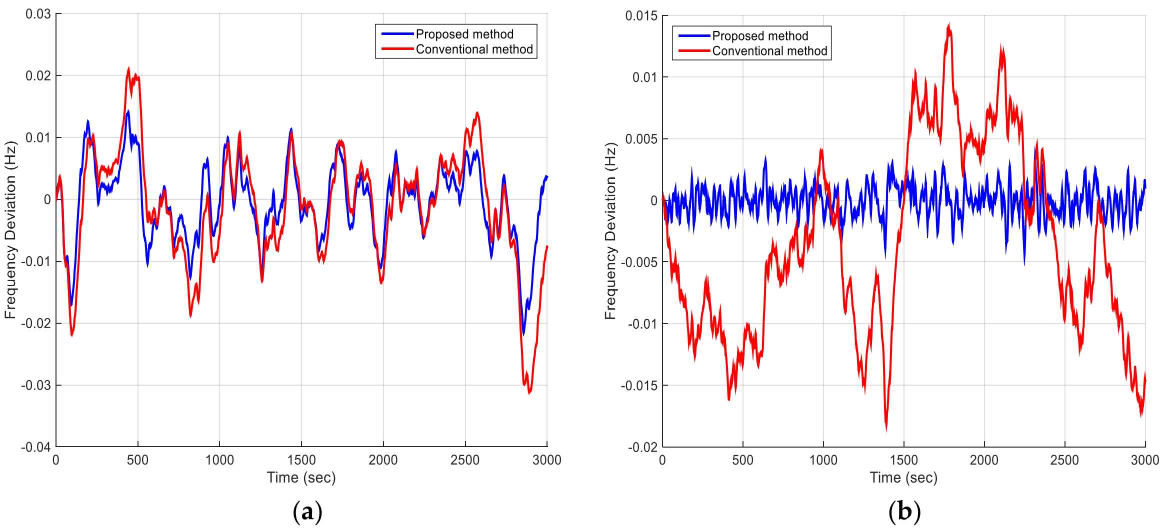

Figure 10. Frequency deviation without disturbance or uncertainties: (**a**) MG_2; (**b**) MG_3.

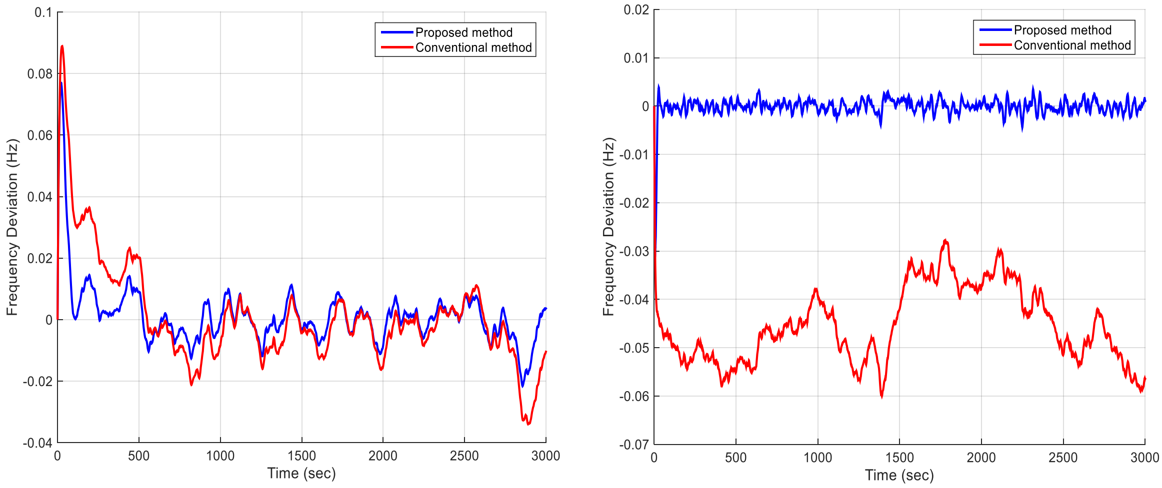

(**a**) (**b**)

Figure 11. Frequency deviation with external disturbance: (**a**) MG_2; (**b**) MG_3.

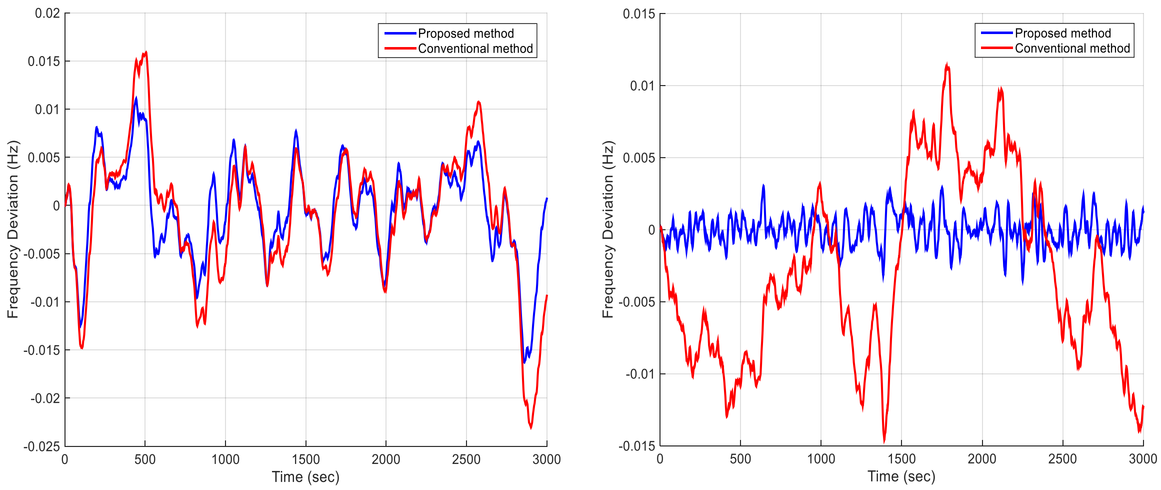

(**a**) (**b**)

Figure 12. Frequency deviation with system parameter uncertainties: (**a**) MG_2; (**b**) MG_3.

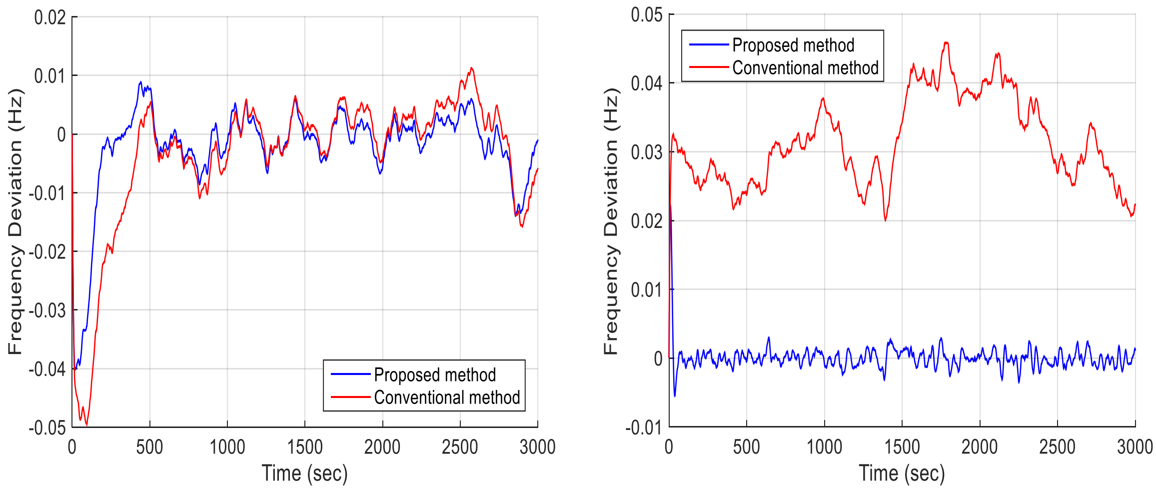

(**a**) (**b**)

Figure 13. Frequency deviation with external disturbance and system parameter uncertainties: (**a**) MG_2; (**b**) MG_3.

Frequency deviation of MG_2 and MG_3 without disturbance or uncertainties are illustrated in Figure 10. Obviously, the proposed method can stabilize the frequency of AC bus in MG_2 and MG_3 more efficiently. When the external disturbance is considered, according to Figure 11, the proposed method has several advantages: the response speed is faster, the overshoot is smaller, and the transition period is shorter than the conventional method. When the system parameters increase by 50%, the frequency deviations of MG_2 and MG_3 are illustrated in Figure 12. The results show the effectiveness of the proposed controller. Moreover, under both external disturbance and system uncertainties, the studied EI system shows better performance with the proposed method, as is shown in Figure 13.

4.2. Comparing the Proposed Controller with the Robust Controller

Second, let the conventional method be only using robust control strategies J_1 in (23) subject to (30).

Figure 14 shows the power transmission between two adjacent MGs under the proposed controller and the conventional robust controller. Power transmission between PG and MG_1 is illustrated in Figure 15. It is obvious that using the proposed method, the transmission power between two adjacent MGs and that between PG and MG_1 can be reduced effectively.

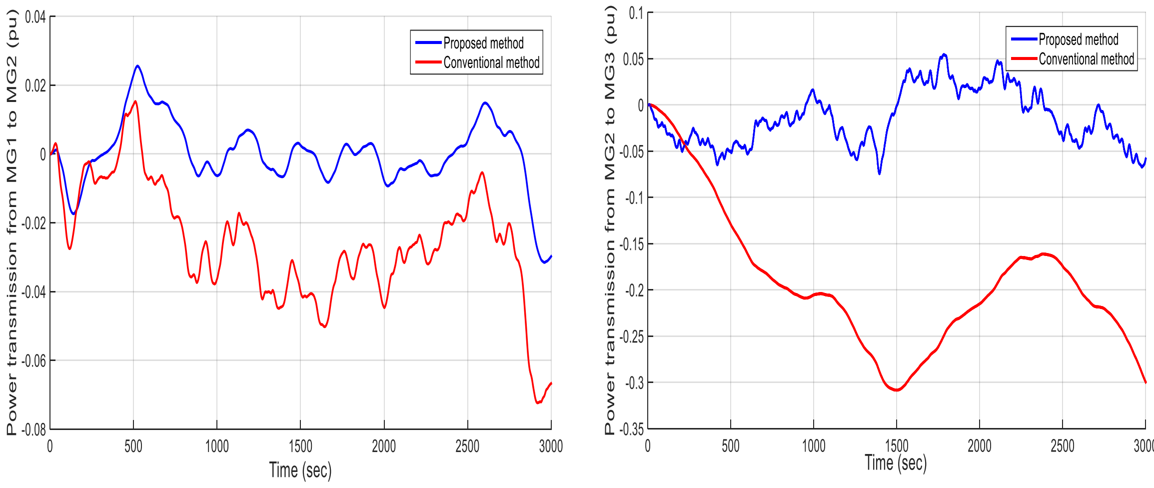

Figure 14. Power transmission between two adjacent MGs. (**a**) Power transmission between MG_1 and MG_2; (**b**) Power transmission between MG_2 and MG_3.

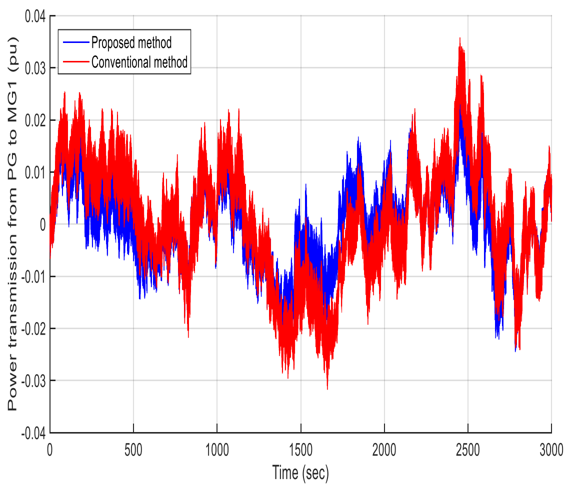

Figure 15. Power transmission between PG and MG_1.

5. Conclusions

In this paper, a class of novel robust and optimal controller design of dynamical series-shaped EI system has been presented. The robustness and operation cost optimization of the EI system are considered simultaneously. PSO algorithm is applied to optimize the parameters of the proposed controller. Simulations show the effectiveness of the proposed method. For our future research, EI system modelling shall be more authentic and complicated, and the system communication time delay shall be taken into consideration.

Author Contributions: The work presented here was carried out through the cooperation of all authors. Haochen Hua and Junwei Cao conceived the scope of the paper; Chuantong Hao and Yuchao Qin conceived the analysis and performed the simulations; Haochen Hua and Chuantong Hao wrote the paper; Junwei Cao acquired the funding and performed revisions before submission. All authors read and approved the manuscript.

Funding: This work was funded in part by National Natural Science Foundation of China (grant No. 61472200) and Beijing Municipal Science & Technology Commission (grant No. Z161100000416004).

Conflicts of Interest: The authors declare no conflict of interest.

References

1. Bhattacharya, M.; Paramati, S.R.; Ozturk, I.; Bhattacharya, S. The effect of renewable energy consumption on economic growth: evidence from top 38 countries. *Appl. Energy* **2016**, *162*, 733–741.
2. Bilgen, S.; Kaygusuz, K.; Sari, A. Renewable energy for a clean and sustainable future. *Energy Sources* **2004**, *26*, 1119–1129.
3. Venkataramanan, G.; Marnay, C. A larger role for microgrids. *IEEE Power Energy Mag.* **2008**, *6*, 78–82.
4. Kroposki, B.; Lasseter, R.; Ise, T.; Morozumi, S.; Papathanassiou, S.; Hatziargyriou, N. Making microgrids work. *IEEE Power and Energy Mag.* **2008**, *6*, 40–53.
5. Mathiesen, B.V.; Lund, H.; Connolly, D.; Wenzel, H.; Østergaard, P.A.; Möller, B. *et al.*, Smart Energy Systems for coherent 100% renewable energy and transport solutions. *Appl. Energy* **2015**, *145*, 139–154.
6. Sreedharan, P.; Farbes, J.; Cutter, E.; Woo, C.; Wang, J. Microgrid and renewable generation integration: University of California, San Diego. *Appl. Energy* **2016**, *169*, 709–20.
7. Odun-Ayo T.; Crow, M.L. Structure-preserved power system transient stability using stochastic energy functions. *IEEE Trans. Power Syst.* **2012**, *27*, 1450–1458.
8. Olivares, D.; Mehrizi-Sani, A.; Etemadi, A.; Canizares, C.; Iravani, R.; Kazerani, M.; *et al.*, Trends in microgrid control. *IEEE Trans. Smart Grid* **2014**, *5*, 1905–1919.
9. Chakrabortty, A.; Ilić, M.D. *Control and Optimization Methods for Electric Smart Grids*, Springer US, 2012.
10. Rifkin, J. *The Third Industrial Revolution: How Lateral Power Is Transforming Energy, The Economy, And The World*, Palgrave Macmillan, New York, 2013; pp. 31–46.
11. Cao J.; Yang, M. Energy Internet - towards smart grid 2.0. In Proceedings of Fourth International Conference on Networking & Distributed Computing, Los Angeles, USA, 2013, 105–110.
12. Tsoukalas L.H.; Gao, R. From smart grids to an energy Internet - assumptions, architectures and requirements. *Smart Grid and Renew. Energy* **2009**, *1*, 18–22.
13. Han, X.; Yang, F.; Bai, C.; Xie, G.; Ren, G.; Hua, H.; Cao, J. An open energy routing network for low-voltage distribution power grid. In Proceedings of 1st IEEE International Conference on Energy Internet, Beijing, China, 2017, 320–325.
14. Geidl, M.; Koeppel, G.; Favre-Perrod, P.; Klokl, B. Energy hubs for the futures. *IEEE Power & Energy Mag.* **2007**, *5*, 24–30.
15. Boyd, J. An internet-inspired electricity grid. *IEEE Spectr.* **2013**, *50*, 12–14.
16. Wu, J.; Guan, X. Coordinated multi-microgrids optimal control algorithm for smart distribution management system. *IEEE Trans. Smart Grid* **2013**, *4*, 2174–2181.
17. Niknam, T.; Azizipanah-Abarghooee, R.; Narimani, M.R. An efficient scenario-based stochastic programming framework for multi-objective optimal micro-grid operation. *Appl. Energy* **2012**, *99*, 455–470.
18. Elrayyah, A.; Cingoz, F.; Sozer, Y. Construction of nonlinear droop relations to optimize islanded microgrid operation. *IEEE Trans. Ind. Appl.* **2015**, *51*, 3404–3413.
19. Zheng, X.; Li, Q.; Li, P.; Ding, D. Cooperative optimal control strategy for microgrid under grid-connected and islanded modes. *Int. J. Photoenergy* **2014**, *2014*, 1–11.

20. Zhao, J.; Dörfler, F. Distributed control and optimization in DC microgrids. *Automatica* **2015**, *61*, 18–26.
21. Bevrani, H.; Feizi, M.R.; Ataee, S. Robust frequency control in an islanded microgrid: H_∞ and μ-Synthesis approaches. *IEEE Trans. Smart Grid* **2016**, *7*, 706–717.
22. Hua, H.; Qin, Y.; Cao, J. Coordinated frequency control for multiple microgrids: a stochastic H_∞ approach, In Proceedings of 2018 IEEE PES Innovative Smart Grid Technologies Asia, Singapore, 2018.
23. Hua, H.; Cao, J.; Yang, G.; Ren, G. Voltage control for uncertain stochastic nonlinear system with application to energy Internet: non-fragile robust H_∞ approach. *J. Math. Anal. Appl.* **2018**, *463*, 93–110.
24. Singh, V.P.; Mohanty, S.R.; Kishor, N.; Ray, P.K. Robust H-infinity load frequency control in hybrid distributed generation system. *Int. J. Elect. Power Energy Syst.* **2013,** *46*, 294–305.
25. Hua, H.; Qin, Y.; Cao, J. A class of optimal and robust controller design for islanded microgrid. In Proceedings of IEEE 7th International Conference on Power and Energy Systems, Toronto, Canada, 2017,111–116.
26. Hua, H.; Qin, Y.; Cao, J.; Wang, W.; Zhou, Q.; Jin, Y.; *et al*., Stochastic optimal and robust control scheme for islanded AC microgrid. In Proceedings of 2018 IEEE International Conference on Probabilistic Methods Applied to Power Systems, Boise, Idaho, US, 2018
27. Vachirasricirikul, S.; Ngamroo, I. Robust LFC in a smart grid with wind power penetration by coordinated V2G control and frequency controller. *IEEE Trans. Smart Grid* **2014**, *5*, 371–380.
28. Shayeghi, H.; Jalili, A.; Shayanfar, H.A. A robust mixed H_2/H_∞ based LFC of a deregulated power system including SMES. *Energy Convers. Manage.* **2008**, *49*, 2656–2668.
29. Ngamroo, I. Robust coordinated control of electrolyzer and PSS for stabilization of microgrid based on PID-based mixed H_2/H_∞ control. *Renew. Energy* **2012**, *45*, 16–23.
30. Farsangi, M.M.; Song, Y.H.; Tan, M. Multi-objective design of damping controllers of FACTS devices via mixed H_2/H_∞ with regional pole placement. *Int. J. Elect. Power and Energy Syst.* **2003**, *25*, 339–346.
31. Kennedy, J.; Eberhart, R. Particle swarm optimization. In Proceedings of IEEE International Conference on Neural Networks, Perth, Australia, 1995, 1942-1948.
32. Zarco, P.; Exposito, A.G. Power system parameter estimation: a survey. *IEEE Trans. Power Syst.* **2002**, *15*, 216-222.
33. Li, X.; Song, Y.J.; Han, S.B. Study on power quality control in multiple renewable energy hybrid microgrid system. In Proceedings of 2007 IEEE Lausanne Power Tech, Lausanne, Switzerland, 2007, 2000-2005.
34. Vachirasricirikul, S.; Ngamroo, I. Robust controller design of heat pump and plug-in hybrid electric vehicle for frequency control in a smart microgrid based on specified-structure mixed H_2/H_∞ control technique. *Appl. Energy* **2011**, *88*, 3860-3868.
35. Gu, D.W.; Petkov, P. H.; Konstantinov, M.M. Robust Control Design with MATLAB, Springer, New York, **2005**.
36. Jiang, Z.P.; Teel, A.R.; Praly, L. Small-gain theorem for ISS systems and applications. *Mathematics of Control Signals & Systems* **1994**, *7*, 95-120.
37. Ho, S.J.; Ho, S.Y.; Hung, M.H.; Shu, L.S.; Huang, H.L. Designing structure-specified mixed H_2/H_∞ optimal controllers using an intelligent genetic algorithm IGA. *IEEE Trans. Control Syst. Technol.* **2005**, *13*, 1119-1124.
38. Asafu-Adjaye J. The relationship between energy consumption, energy prices and economic growth: time series evidence from Asian developing countries. In Proceedings of Australian Agricultural and Resource Economics Society, 1999, 615-625.
39. Hang, L.; Tu, M. The impacts of energy prices on energy intensity: evidence from China. *Energy Policy* **2007**, *35*, 2978-2988.
40. Kirschen, D.S.; Strbac, G.; Cumperayot, P. Factoring the elasticity of demand in electricity prices. *IEEE Trans. Power Syst.* **2000**, *15*, 612-617.
41. Carpinelli, G.; Mottola, F.; Proto, D. A multi-objective approach for microgrid scheduling. *IEEE Trans. Smart Grid* **2017**, *8*, 2109-2118.